

Impact of photometric redshifts on the galaxy power spectrum and BAO scale in the LSST survey

Reza Ansari¹, Adeline Choyer², Farhang Habibi¹, Christophe Magneville³, Marc Moniez¹, Stéphane Plaszczyński¹, Cécile Renault^{2*}, Jean-Stéphane Ricol², and Julien Souchard²

¹ LAL, Univ. Paris-Sud, CNRS/IN2P3, Université Paris-Saclay, Orsay, France

² Univ. Grenoble Alpes, CNRS, Grenoble INP, LPSC-IN2P3, 38000 Grenoble, France

³ DSM/Irfu/SPP, CEA-Saclay, F-91191 Gif-sur-Yvette Cedex, France

Received DD MM 2018/ Accepted DD MM 2018

ABSTRACT

Context. Imaging billions of galaxies every few nights during ten years, LSST should be a major contributor to precision cosmology in the 2020 decade. High precision photometric data will be available in six bands, from near-infrared to near-ultraviolet. The computation of precise, unbiased, photometric redshifts up to $z = 2$, at least, is one of the main LSST challenges and its performance will have major impact on all extragalactic LSST sciences.

Aims. We evaluate the efficiency of our photometric redshift reconstruction on mock galaxy catalogs up to $z=2.45$ and estimate the impact of realistic photometric redshift (hereafter photo- z) reconstruction on the large-scale structures (LSS) power spectrum and the baryonic acoustic oscillation (BAO) scale determination for a LSST-like photometric survey. We study the effectiveness of the BAO scale as a cosmological probe in the LSST survey.

Methods. We have performed a detailed modelling of the photo- z distribution as a function of galaxy type, redshift and absolute magnitude using our photo- z reconstruction code with a quality selection cut based on a Boosted decision tree (BDT). We simulate a catalog of galaxies in the redshift range $[0.2 - 2.45]$ using the Planck 2015 Λ CDM cosmological parameters over 10,000 square-degrees, in the six *ugrizy* bands, assuming LSST photometric precision for a ten-year survey. The mock galaxy catalogs are produced with several redshift error models. The LSS power spectrum is then computed in several redshift ranges and for each error model. Finally we extract the BAO scale and its uncertainty.

Results. We have computed the fractional error on the recovered power spectrum $\sigma[P(k)]/P(k)$ which is dominated by the shot-noise at high redshift ($z \gtrsim 1$), for scales $k \gtrsim 0.1$, due to the photo- z damping. The BAO scale can be recovered with an accuracy of about a percent from $z = 0.5$ to $z = 1.5$ using realistic photo- z reconstruction. Outliers (*i.e.* galaxies with catastrophic photo- z) can represent a significant fraction of galaxies at high redshift ($z \gtrsim 2$), causing bias and errors on LSS power spectrum measurement.

Conclusions. Reaching the LSST requirements for photo- z reconstruction is crucial to exploit the LSST potential in cosmology, in particular to measure the LSS power spectrum and its evolution with redshift. Although the BAO scale is not the most powerful cosmological probe in LSST, it can be used to check the consistency of the LSS measurement. Moreover we show that despite the photo- z smearing, the isotropic BAO scale determination in LSST remains competitive with future spectroscopic surveys.

Key words. Galaxies: distances and redshifts – Galaxies: photometry – Cosmology: large-scale structure of Universe – Cosmology: dark energy

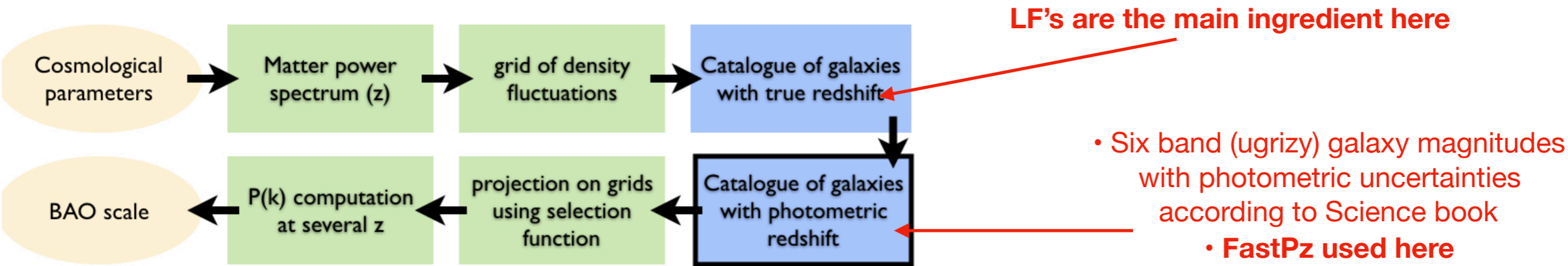
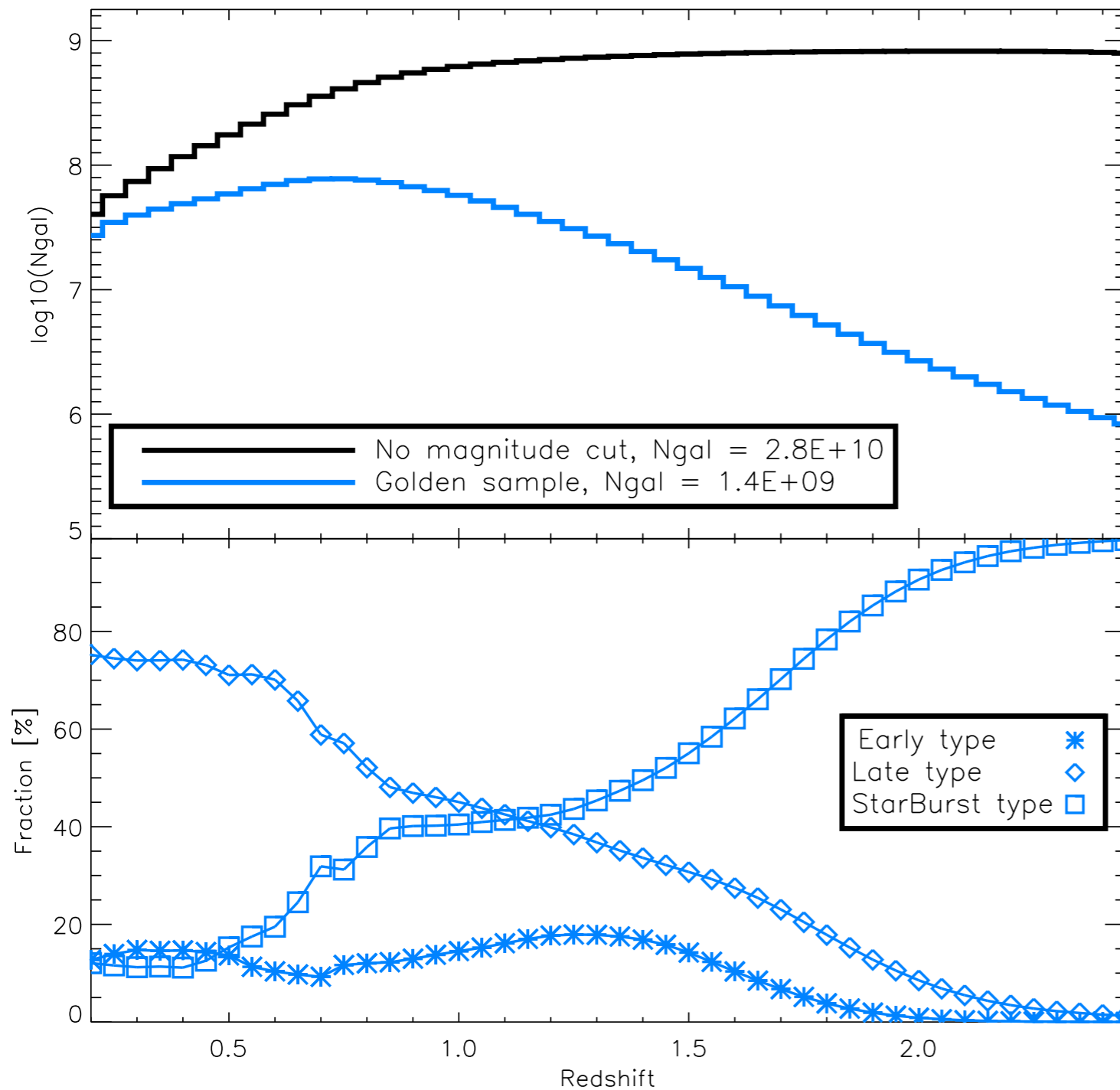


photo-Z by template fitting

Main issues studied that affect the LSS PS estimation

- The galaxy number density and its evolution with redshift
- Reconstructed photo-z quality (dispersion, outliers ...)
- The damping effect introduced by photo-z smearing and additional noise due to outliers



**Base selection cut :
LSST golden sample
galaxies with $i < 25.3$**

**1.4 10^9 galaxies from with
 z_s in [0.2-2.45]**

Fig. 3. Top: Number of galaxies per redshift interval. The *LSST golden selection cut* is defined by $m_i < 25.3$. Bottom: relative distribution of the broad types of the galaxies satisfying the *LSST golden selection cut* as a function of the redshift.

**Use of (Zucca et al., 2009) LF
instead of (Dahlen et al, 2005) LF**
 —> better behaviour n_{type} / z
 —> number density in better
 agreement with HSC

photo-Z

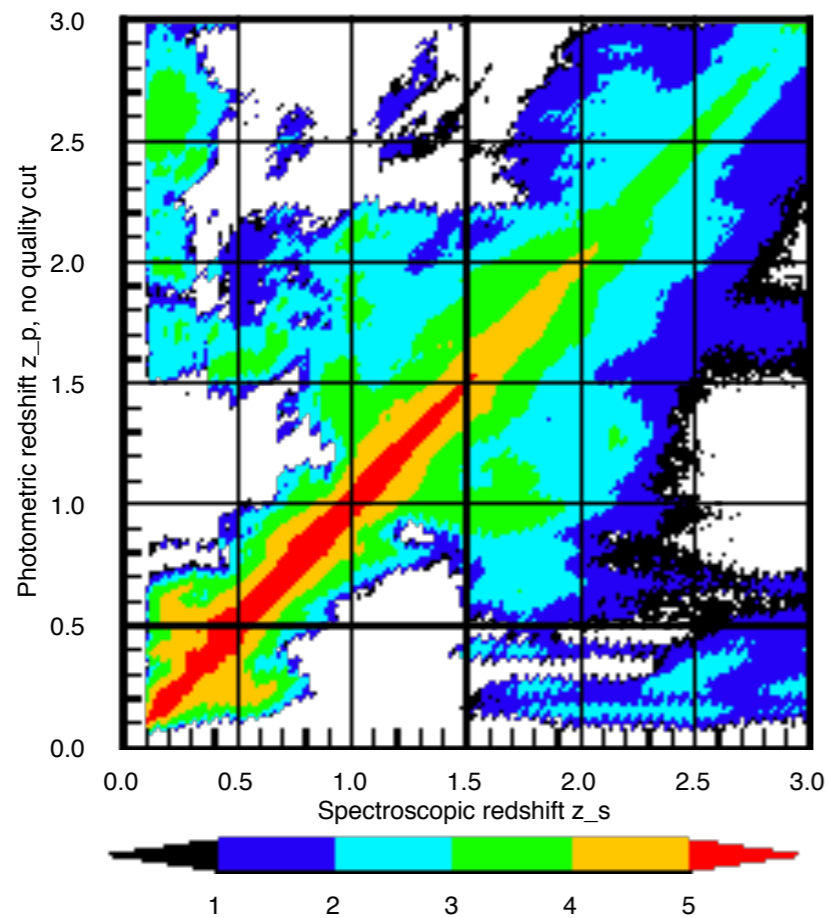
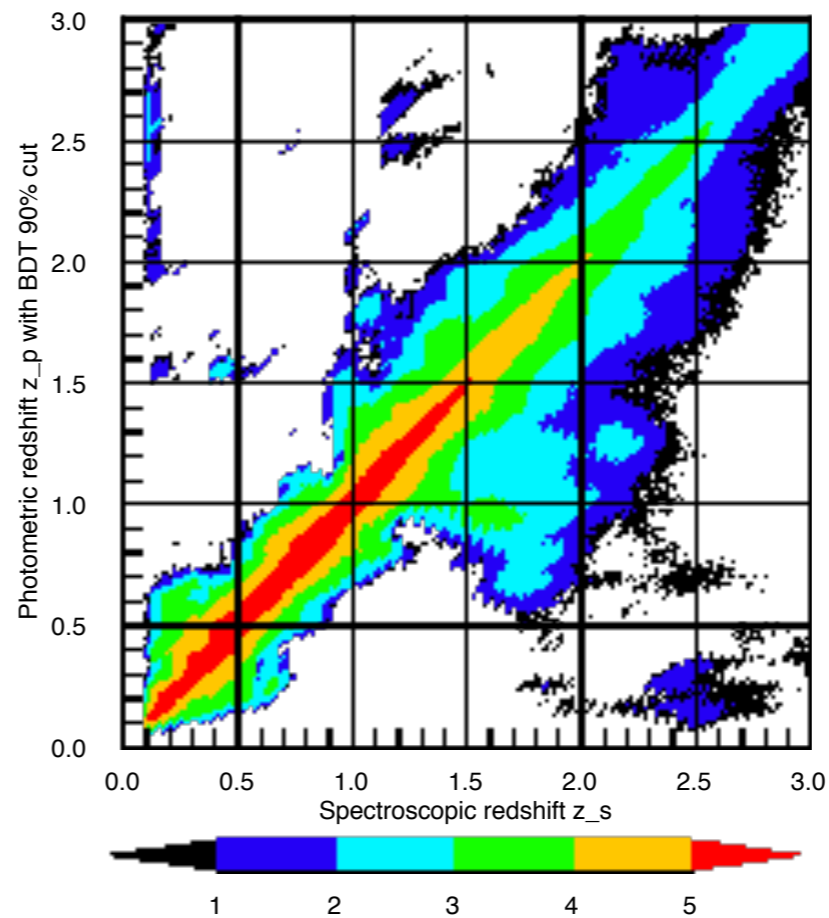
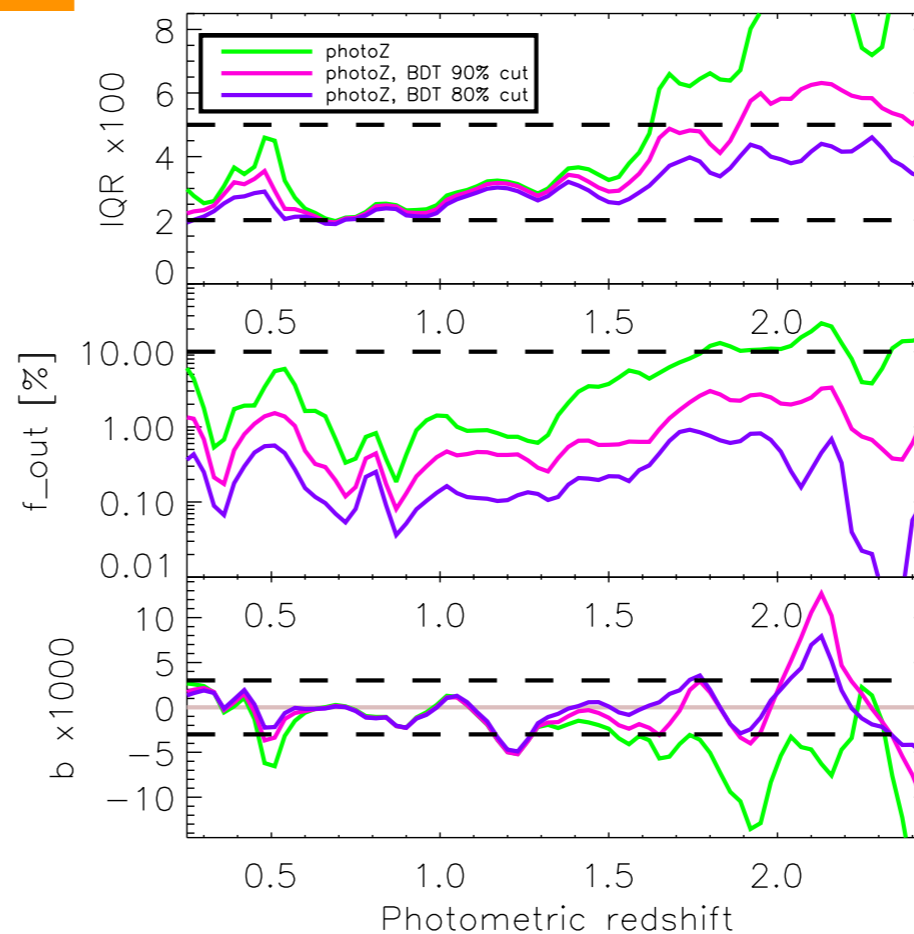
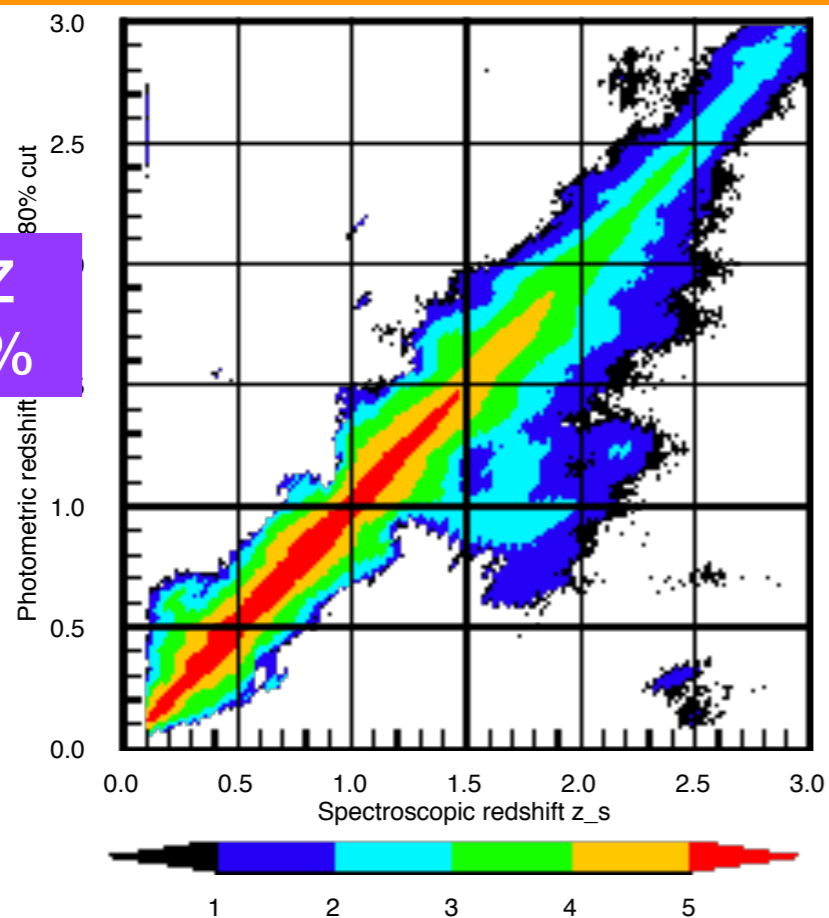


photo-Z
BDT 90%



The colour scale for the galaxy density is logarithmic

photo-Z
BDT 80%



IQR (= 1.3 sigma)

outliers

bias

Outliers and selection function

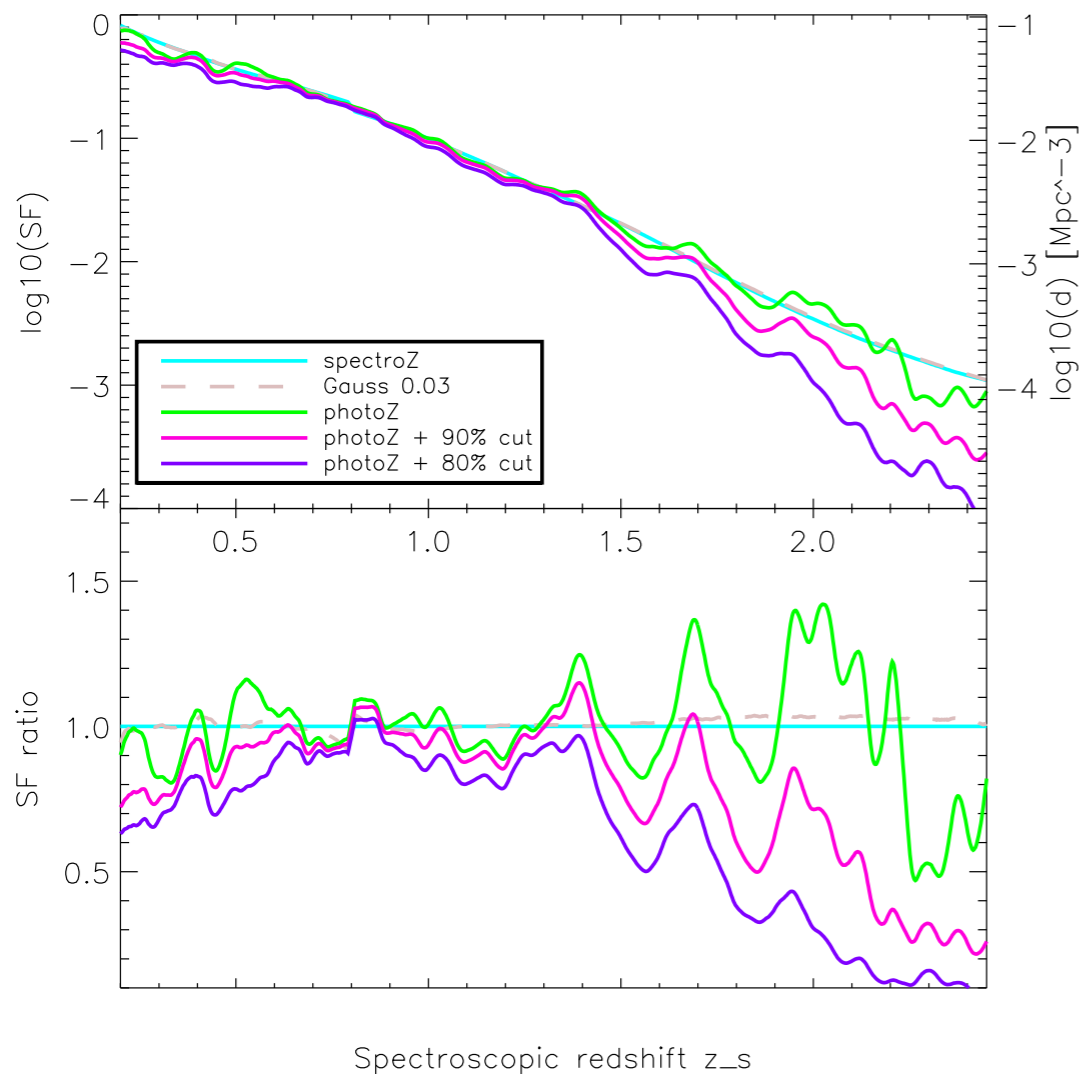


Fig. 5. Selection functions SF in the redshift range [0.2-2.45], using the various estimations of the redshift. Top: selection functions defined as the ratio between the number of galaxies in the catalog (passing the *LSST golden selection cut*) and the number of simulated galaxies. The right axis gives the galaxy density d per Mpc^{-3} . Bottom: ratio between the selection functions and the selection function in the spectroscopic case.

photo-Z introduces wiggles in the selection function (systematic shifts)

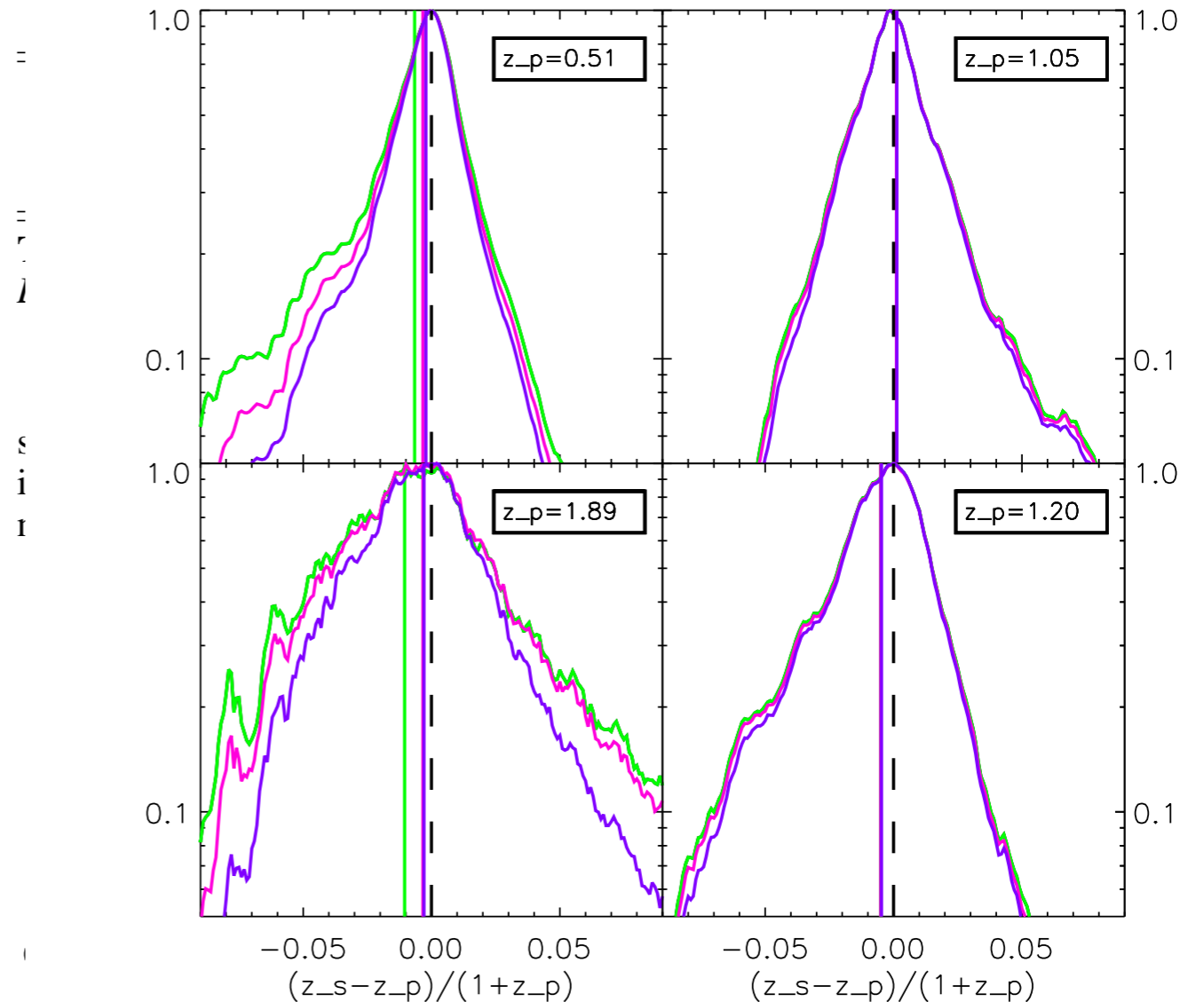


Fig. 6. Normalised histogram of $e_z = (z_s - z_p)/(1 + z_p)$ for 4 bins in photo-z. The coloured vertical lines show the value of the bias for the 3 error models on the photo-z considered (see Fig. 5 for colour legend) while the dashed black line is the reference at 0.

bias are not link to a shift but to an asymmetry in $(z_s - z_p)/(1 + z_p)$ —> should not be corrected for

z range	0.2-0.5	0.5-1.0	1.0-1.5	1.5-2.5	0.2-2.5
$z = z_G$	6.7	19.0	9.3	2.5	37.5
$z = z_p$	6.2	19.7	9.3	2.4	37.6
$z = z_{\text{BDT90}}$	5.5	18.6	8.8	1.7	34.6
$z = z_{\text{BDT80}}$	4.9	17.4	8.0	1.1	31.4

Table 1. Number of galaxies per arc-min² per redshift range. The *LSST golden selection cut* is always applied.

f_{gal} with	$ e_z < 0.02$	$ e_z < 0.05$	$ e_z < 0.15$
for $z = z_G$	49 %	90 %	100 %
for $z = z_p$	61 %	85 %	97 %
for $z = z_{\text{BDT9}}$	65 %	89 %	99 %
for $z = z_{\text{BDT8}}$	68 %	91 %	100 %

Table 2. Fraction of galaxies f_{gal} with $|e_z| = |z_s - z_p| / (1 + z_p)$ lower than several thresholds for the three photometric error models. The threshold of 0.02 is the goal, 0.05 is the requirement ; 0.15 defines the outliers.

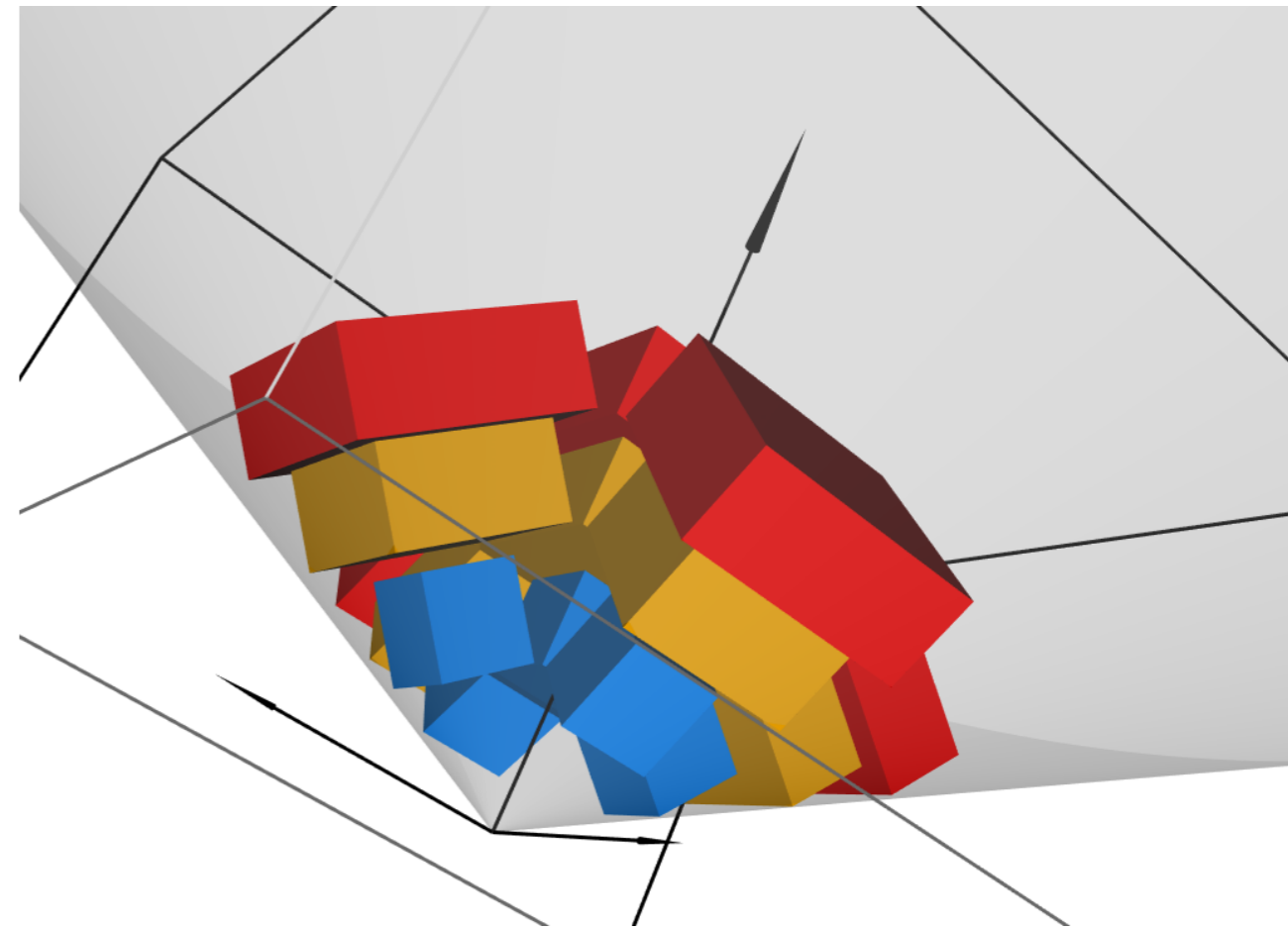


Fig. 7. Schematic view of the volumes used in the simulation. The black lines mark out the *BigCube*. The grey area shows the field of view of π sr which is filled by galaxies from $z = 0.2$ to $z = 2.45$. The 5 grids used to compute each power spectrum are drawn in blue, orange or red according to their central redshift.

grids where galaxies are projected

$z=0.5$

$z=0.9$

$z=1.3$

Smearing and damping due to photo-Z

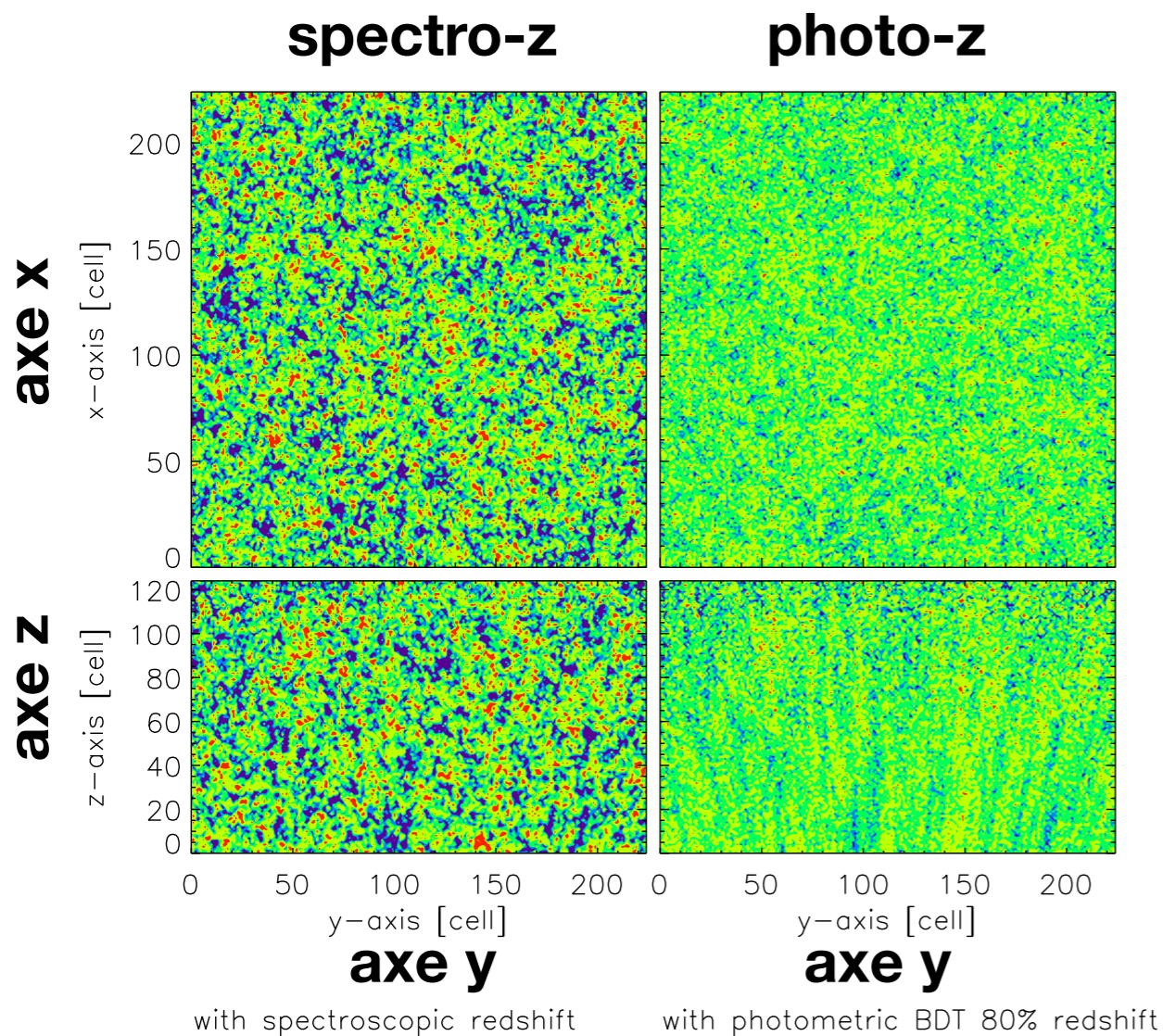


Fig. 8. Galaxy density contours in slices of the grid centred at $z = 0.9$. Top: the transverse plane (y, x); bottom: the radial plane (y, z). Left : with spectro-z, right : with BDT 80% photo-z. Slices are 8 comoving Mpc thick (1 cell) and go through the grid center.

damping when photo-z are used (even Gaussian)

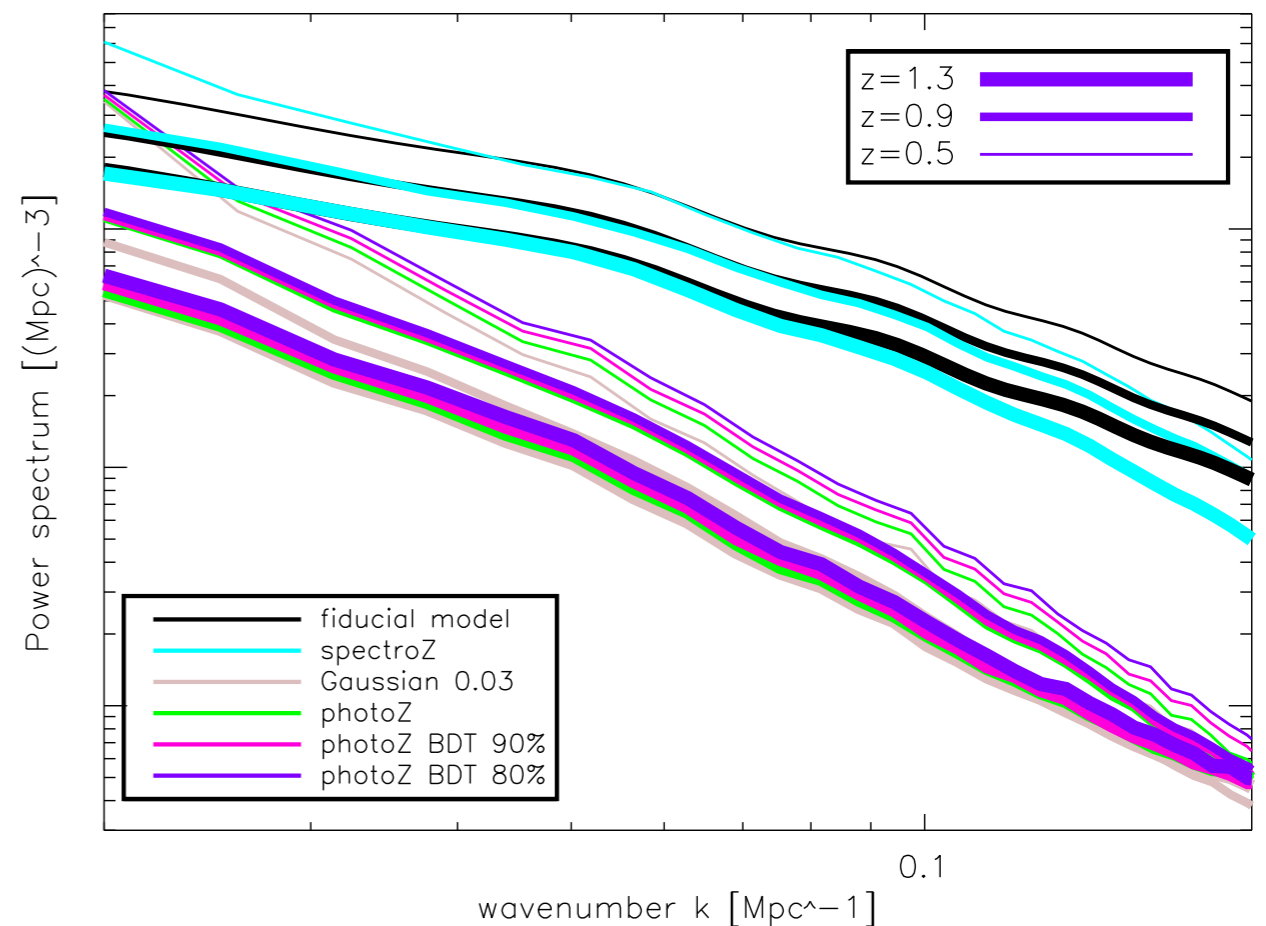
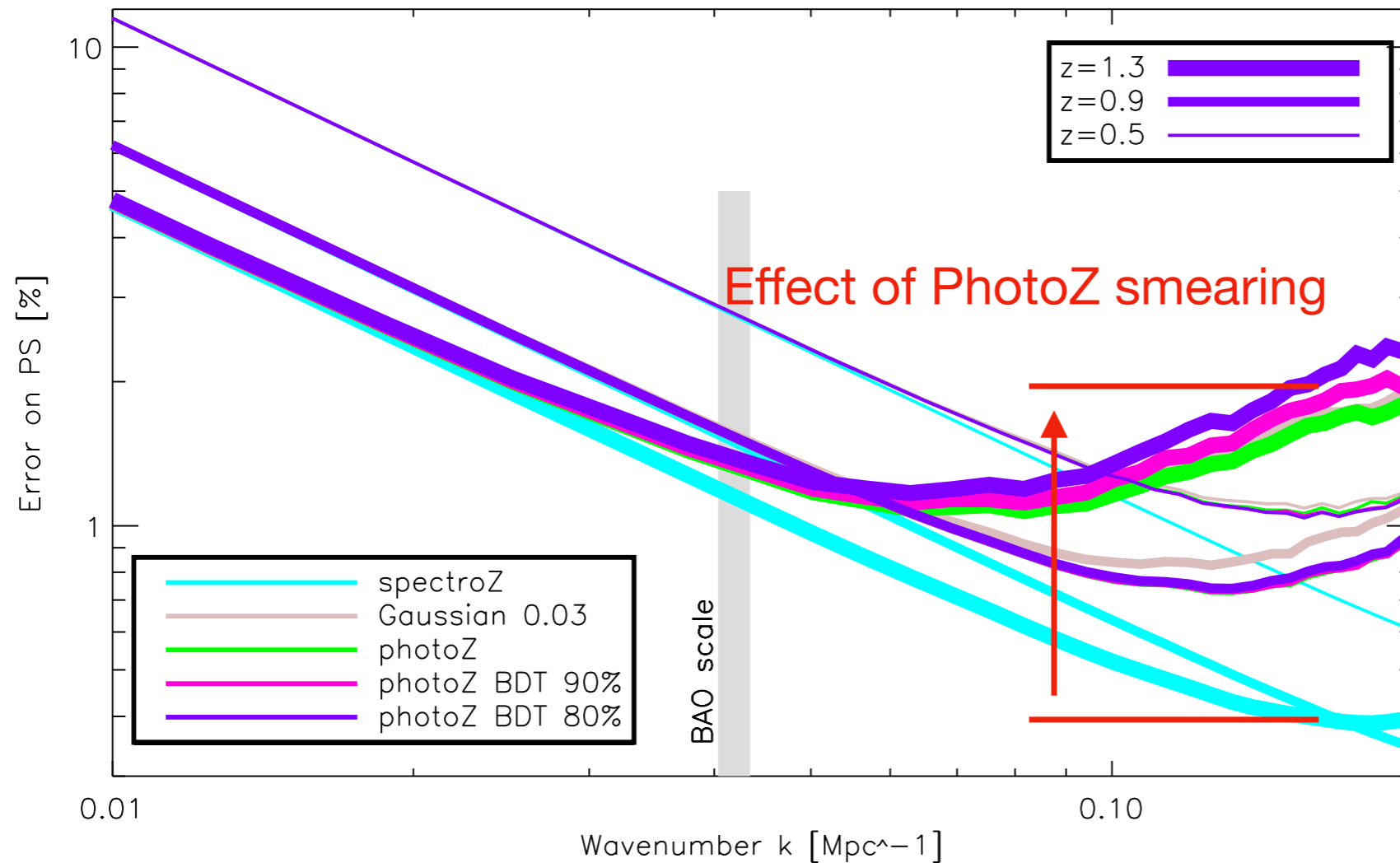


Fig. 9. Recovered power spectra $P_D(k)$ computed from the 5 grids centred at each redshift bin, after subtraction of the shot-noise contribution. Black lines correspond to the theoretical (input) power spectra while other colours refer to the five redshift error models. The line thickness identifies the grids central redshift, with the thickness increasing with the redshift.

Photo-Z induced damping impacts the fractional error



→ compare cyan and purple curves of same thickness

At high z, damping has an impact already at the BAO scale

Fig. 10. Fractional statistical error $\sigma_P/P(k)$ of the recovered power spectra P_D in percent. Colors identify the different redshift error models, while the grid redshifts are distinguished by different line thicknesses. The light gray area shows the wave number corresponding to the BAO scale.

BAO scale uncertainty (lower limits on s_A)

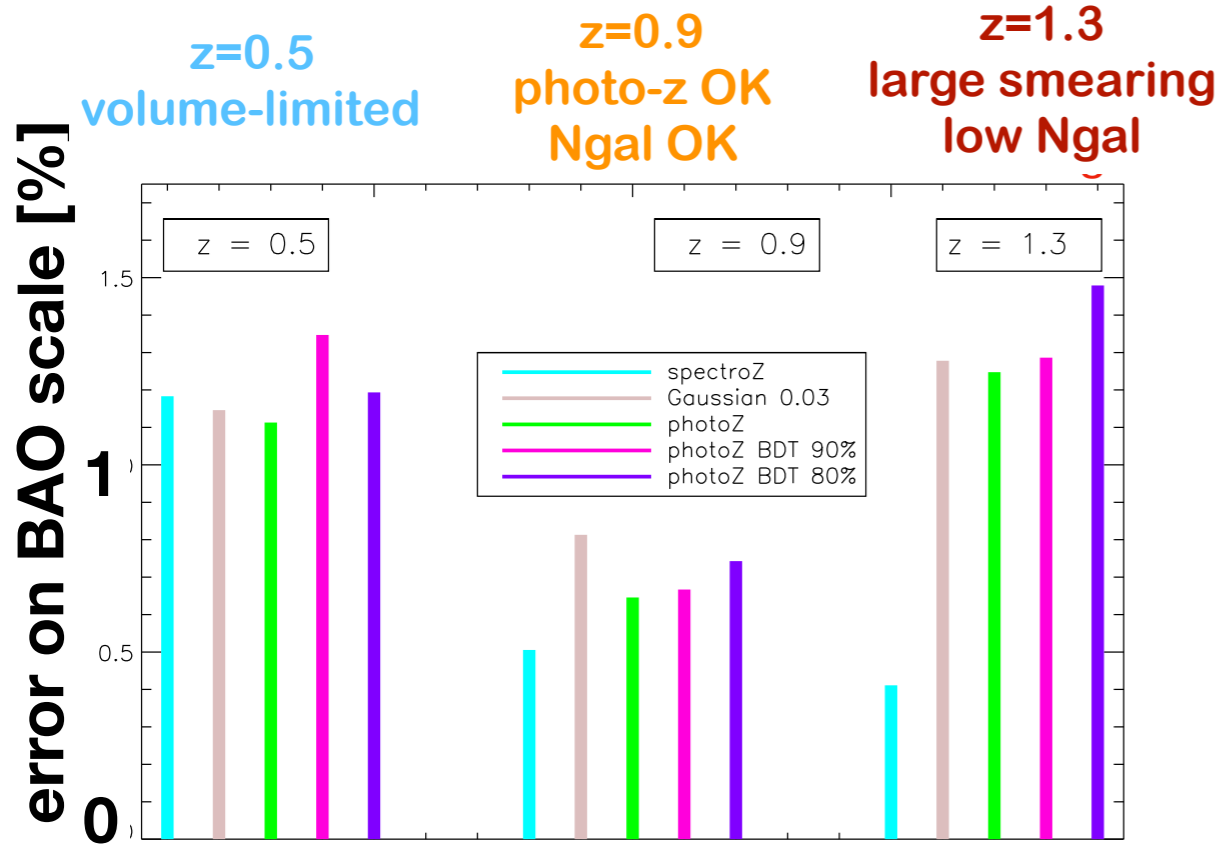


Fig. 12. Relative errors on the BAO scale fitted from the power spectra for each redshift and each error model.

full simulation with multiple grids, around
4000 deg² effective analysis area

redshift [z_{min}, z_{max}]	Photometric survey			Spectroscopic survey	
	\bar{n}_{gal} [10^{-3}]	σ_{s_A} [%] with z_s	σ_{s_A} [%] with z_p	\bar{n}_{gal} [10^{-5}]	σ_{s_A} [%]
[0.4 – 0.7]	15	0.3	0.4	30	0.5
[0.7 – 1.0]	10	0.2	0.3	20	0.5
[1.0 – 1.3]	6	0.2	0.4	12	0.6
[1.3 – 1.6]	3	0.2	0.5	6	0.8
[1.6 – 1.9]	1.3	0.2	0.7	4	1.1
[1.9 – 2.2]	0.6	0.3	1.4	2	1.8

Table 4. Lower limits for BAO scale determination uncertainty σ_{s_A} in Mpc for different redshift ranges, for an LSST like photometric survey (left), and for a DESI like spectroscopic survey (right) with $\Omega_{surv} = 10,000 \text{ deg}^2$. \bar{n}_{gal} is the galaxy number density. Notice that galaxy number densities are given in units of 10^{-3} Mpc^{-3} for the photometric survey and 10^{-5} Mpc^{-3} for the spectroscopic survey. As previously, z_s stands for the use of spectro-z and z_p for the use of photo-z with errors similar to the reconstructed photo-z with the BDT 90% quality cut.

galaxy density (n_{gal}) not large enough to compensate Photo-z smearing - BAO signal washed out gradually

Next steps / work direction

- Move to DESC tools and simulations
- Use spherical shells and evaluate separately radial and transverse BAO scales and associated errors
- At low redshift ($z \sim 0.5$), try to identify sub sample of galaxies with good photo- z
- Work on systematic effects affecting $n_{\text{gal}}(z)$ and photo- z : dust ...
- Work on SED templates for simulations and photo- z (FORS2 templates (E. Nuss, J. Cohen-Tanuji ...))
- Use Johanna's photo- Z method